Original Article

A precise surgical planning system for hepatectomy coupled with liver tissue in the hepato-portal vein territories

Mengna Zhang[1#], Chengbin Peng[2#], Ying'an Zhao[3], Yuting Hong[2], Guofeng Zhu[2], Shi Ying[4], Bin Zhang[3], Xuanlei Ren[3], Jiyun Zhu[3], Jianbo Zheng[3], Zehao Yu[3], Yufei Chen[5], Siming Zheng[3]

[1]Department of Hepatobiliary and Pancreatic Surgery, The First Affiliated Hospital, Zhejiang University School of Medicine, Zhejiang University, Hangzhou, China; [2]College of Information Science and Engineering, Ningbo University, Ningbo, China; [3]Department of Hepatobiliary and Pancreatic Surgery, The First Affiliated Hospital of Ningbo University (Ningbo Hospital, Zhejiang University), Ningbo, China; [4]Ningbo Wedge Medical Technology Co., LTD., Ningbo, China; [5]College of Electronic and Information Engineering, Tongji University, Shanghai, China

Contributions: (I) Conception and design: S Zheng, C Peng; (II) Administrative support: S Zheng; (III) Provision of study materials or patients: S Zheng, S Ying, B Zhang, X Ren, J Zhu, J Zheng, Z Yu, Y Chen; (IV) Collection and assembly of data: M Zhang, Y Zhao, Y Hong, G Zhu, S Ying; (V) Data analysis and interpretation: M Zhang, Y Zhao, C Peng, S Ying; (VI) Manuscript writing: All authors; (VII) Final approval of manuscript: All authors.

[#]These authors contributed equally to this work as co-first authors.

Correspondence to: Siming Zheng, MD. Department of Hepatobiliary and Pancreatic Surgery, The First Affiliated Hospital of Ningbo University (Ningbo Hospital, Zhejiang University), Hepatobiliary and Pancreatic First Ward, 16F, Building 2, No. 59 Liuting Street, Ningbo 315000, China. Email: 29010921@qq.com.

Background: With the advancement of precise hepatic resection and three-dimensional (3D) reconstruction technology, there is a growing emphasis on precision in liver surgery. However, during hepatic resection, thick hepatic veins may appear in the portal vein basin, and injury to thick hepatic veins may cause residual hepatic stasis, resulting in impaired liver function, or even failure. Therefore, we developed a new computer-assisted hepatic surgical planning system that integrates the portal and hepatic vein basins. This system is designed to achieve oncological safety and preserve functional hepatic tissues by reducing ischemic volume (IV), congested volume (CV), and transection surface area (TSA), leaving the residual liver with less ischemic volume, sludge volume, and cross-sectional area, thereby optimizing postoperative outcomes.

Methods: Contrast-enhanced computed tomography (CT) datasets from 20 patients at The First Affiliated Hospital of Ningbo University were analyzed for 3D reconstruction. Using a pseudorandom number generator algorithm, 140 liver occupancy models were established with seven points selected from each case. Three distinct surgical simulation strategies were compared: hepatic-portal venous territory integration, anatomical portal territory resection, and non-anatomical resection (NAR) (1-cm margin), the liver occupancy models were compared with the three types of surgical planning. Quantitative parameters, including Resected Index (RI, resected volume/total liver volume), Ischemic Index (II, residual ischemic volume/total liver volume), Congestion Index (CI, residual CV/total liver volume), and transection surface ratio (TSR, cross-sectional area/total liver surface area), were analyzed to evaluate the value of the surgical planning system.

Results: Compared with portal vein basin anatomical hepatectomy, the integrated method had smaller RI [8.09 (3.00, 20.12) *vs.* 18.9 (2.84, 42.29), P<0.05], CI [1.14 (0.37, 3.68) *vs.* 3.39 (0.35, 13.26), P<0.05], II [2.28 (0.82, 7.10) *vs.* 3.39 (0.35, 13.26), P<0.05], and TSR [14,417.13 (7,462.02, 32,715.68) *vs.* 73,739.52 (47,559.78, 102,632.74), P<0.05]. When compared to NAR, the integration strategy achieved reduced II [1.15 (0.46, 3.43) *vs.* 7.63 (3.00, 24.16), P<0.05], CI [1.14 (0.37, 3.68) *vs.* 7.67 (2.16, 22.98), P<0.05], and RI [2.28 (0.82, 7.10) *vs.* 15.28 (4.46, 47.14), P<0.05].

Conclusions: In this study, we established a surgical planning system coordinating portal perfusion

© AME Publishing Company.

territories with hepatic venous drainage basins. The computational planning system significantly improves surgical precision by reducing residual ischemic volume, venous congestion, and parenchymal transection area.

Keywords: Surgical planning system; hepatectomy; hepato-portal vein territories; three-dimensional visualization; voxelization

Submitted Oct 27, 2024. Accepted for publication Mar 27, 2025. Published online Apr 28, 2025.
doi: 10.21037/qims-24-2349
View this article at: https://dx.doi.org/10.21037/qims-24-2349

Introduction

Surgical resection remains the primary treatment for liver cancer. Due to the liver's complex internal architecture, precise preoperative assessment of lesion locations and vascular distributions is crucial to enhancing surgical accuracy and success rates. Couinaud segmentation often contradicts actual surgical findings and radiological research (1). Alternative liver segmentation methods proposed by Takasaki and Cho *et al.* (2,3), along with Fasel's "1-2-20 concept" identifying 20 second-order portal branches within the portal vein, have advanced our understanding of hepatic vascular anatomy (4). Contemporary three-dimensional (3D) reconstruction technologies now enable portal territory analysis based on liver tumor dissemination patterns along the portal vein, facilitating resection precision at the lobar, segmental, subsegmental, and even jigsaw puzzle levels. However, thick hepatic veins can be present in these territories, and damaging these veins may lead to residual liver congestion, impairing liver function or causing liver failure.

Although traffic veins in a portion of the liver can compensate for the return of hepatic parenchyma in resected territories (5), their compensatory capacity is primarily limited to scenarios necessitating major hepatectomy such as multiple tumors in the liver or obstruction of principal hepatic veins. The present study focuses on lobular, segmental, subsegmental, and jigsaw hepatectomies; traffic veins are not typically observed in cases requiring such surgical interventions.

To optimize hepatic surgical resection and preserve functional hepatic tissue, we developed a new computer-assisted hepatic surgical planning system that integrates the effects of the portal and hepatic vein basins. This system allows surgeons to preserve maximal functional parenchymal volume with minimized ischemic burden and venous congestion in the residual liver while reducing transection surface area (TSA) and ensuring oncologic safety.

Methods

Data and grouping

This study enrolled 20 patients at The First Affiliated Hospital of Ningbo University who met the following inclusion criteria: (I) absence of underlying comorbidities; (II) normal hepatic morphology without chronic pathology; (III) patent portal venous system; (IV) high quality CT image quality permitting clear visualization of liver and intrahepatic vessels as well as tertiary and quaternary portal/hepatic venous branches. These participants underwent multiphase 256-slice contrast-enhanced CT (non-contrast, arterial, portal venous, and hepatic venous phase) with layer thickness of 0.6 mm. This study was conducted in accordance with the Declaration of Helsinki and its subsequent amendments under approval from the Ethics Committee of The First Affiliated Hospital of Ningbo University (No. 2021-R138). Informed consent was provided by all participants.

Digital Imaging and Communications in Medicine (DICOM) datasets were processed through the InsideView-Liver 3D Reconstruction System (Zhejiang Medical Device Reg. No. 20222210138) by a radiologist and a 3D reconstruction engineer who jointly conducted the registration and 3D reconstruction of the image data in each phase.

A random number generation algorithm (6) was used to generate seven random points from each patient-specific 3D liver model (n=20), creating 140 liver space-occupying models (10-mm spherical volumes of interest). Models demonstrating proximity <1 cm to primary and secondary branches of portal vein or hepatic vein were excluded. All 140 models were subjected to three surgical simulations

© AME Publishing Company.

[hepatic-portal venous territory integration, anatomical portal territory resection, and 1-cm margin non-anatomical resection (NAR)] to obtain a study group, anatomical resection (AR) group, and NAR group, respectively.

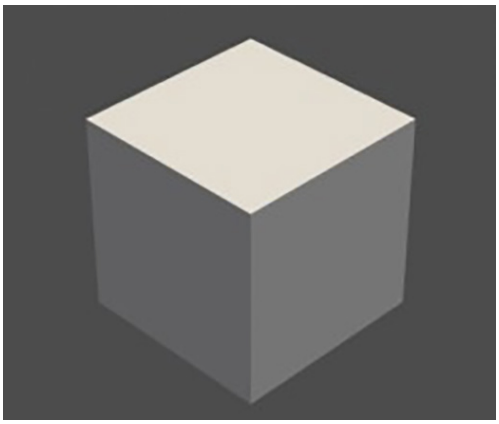

Figure 1 Voxel blocks.

Algorithms and related concepts

Voxelization

The reconstructed hepatic models underwent voxelization with the voxel block defined as a cube with a side length of 1 mm (*Figure 1*), where each voxel block's spatial coordinates were represented by the coordinates of its center in the 3D space. In voxelization, various voxel blocks were used to represent liver parenchyma, liver space-occupying lesions, and hepato-portal vein respectively, to jointly build the 3D model of the liver (*Figure 2*).

Vascular tree model

To describe the vascular connection, this paper introduces a vascular tree model based on a linked list (*Figure 3*). The sequence of vascular voxel blocks was recorded by flood filling from vessel origins, and the front and rear voxel blocks were connected with a linked list. This model is implemented as follows:

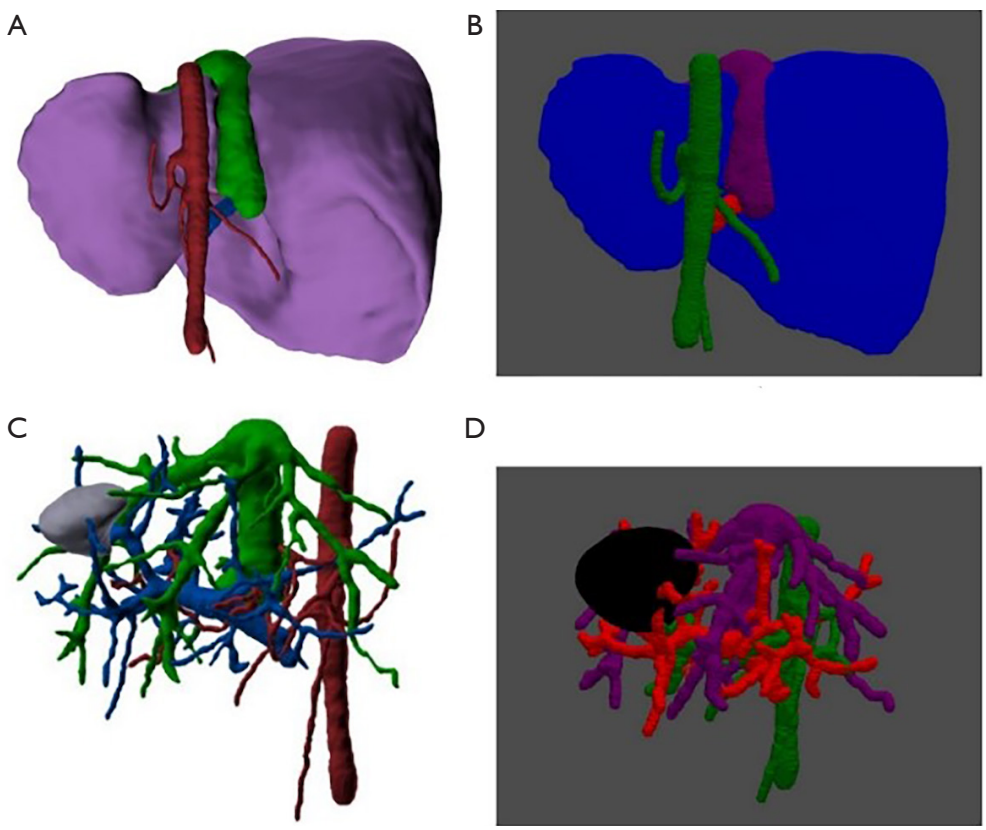

Figure 2 Voxelization results. (A) Liver parenchyma. (B) Voxelized liver parenchyma. (C) Blood vessels and tumor. (D) Voxelized blood vessels and tumor.

© AME Publishing Company.

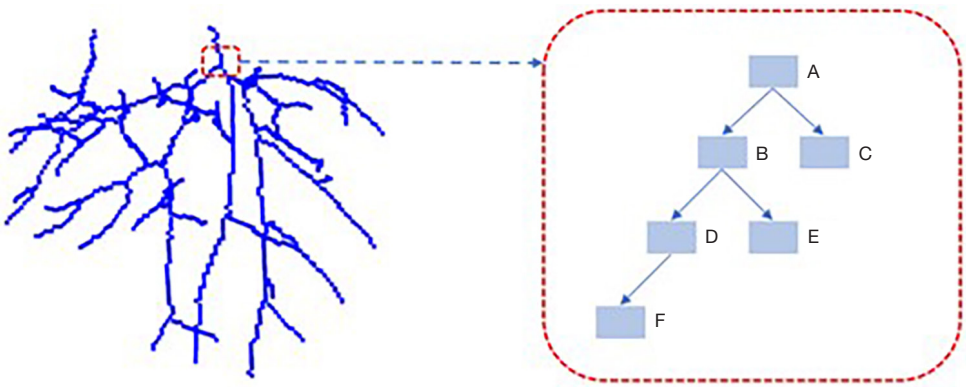

Figure 3 An example of the construction of a linked list model describing a vascular tree. A, the root of the vascular tree; B,D, the middle part of the vessel; C,E,F, the terminal branches of the vessel.

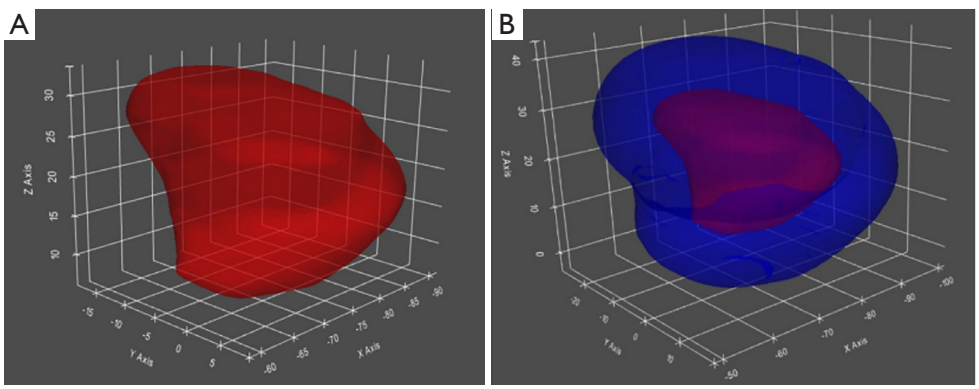

Figure 4 Liver space-occupying and 1 cm expansion effect. (A) Initial occupancy. (B) Expanded cut edge.

(I) Evaluate the importance of vascular voxel blocks in different locations by recording the number of liver parenchyma voxel blocks supplied by each vascular voxel block;
(II) When there is hepatic parenchyma to be resected, the number of hepatic parenchyma voxel blocks controlled by vascularization voxel blocks is updated through the vascular tree.

On this basis, simulated surgery was performed on 140 liver-occupying models by applying three surgical methods respectively in the (I) study group, (II) AR group, and (III) NAR group. Quantitative outcomes were assessed by calculating Resected Index (RI, resected volume/total liver volume), Ischemic Index (II, residual ischemic volume/total liver volume), Congestion Index [CI, residual congested volume (CV)/total liver volume], Composite Residual Index (CRI, residual ischemic + congested liver parenchymal volume/total liver parenchymal volume), and transection surface ratio (TSR, cross-sectional area/total liver surface area). The resected liver parenchyma volume/total liver parenchyma volume, residual ischemic liver parenchyma volume/total liver parenchyma volume, residual congested parenchyma liver volume/total liver parenchyma volume, residual ischemic + congested liver parenchymal volume/total liver parenchymal volume, and liver cross-sectional area were calculated in the three groups to evaluate the differences of the three surgical modalities mentioned above, and to explore the value of the integration approach.

Study group (hepatic-portal vein basin coupling)

Overall goal: To achieve radical resection of the occupying lesion (7). The lesion surface was expanded outward by 1 cm to establish the initial resection margin (*Figure 4*). Subsequent iterative 1 mm^3 voxel-wise expansions were performed with each step selecting the spatially adjacent unit exhibiting minimal composite resection weight by the

© AME Publishing Company.

following five indexes: RI, II, CI, CRI, and TSR. The vascular structure and candidate regions were also dynamically updated, and the process was continuously iterated until the resection weights of all candidate spatial units were less than zero.

Specific processes:

(I) Space occupation expansion

We expanded and resected the hepatic occupancy by 1 cm based on the vertex normal vector (8), and the remaining liver was the area to be resected, where the spatial units neighboring the margin of dissection formed the candidate resection area.

(II) Comprehensive scoring of the proposed excision space units using a weighting function

The spatial units in the candidate resection area include two kinds: (a) vascular spatial units: all the spatial units within 1×1×1 mm^3 are vascular components; (b) hepatic parenchymal spatial units: all the spatial units within 1×1×1 mm^3 are hepatic parenchymal components.

(i) Calculation of the importance of vascular voxel blocks:

- g function: calculate the importance of a given hepatic vein vascular voxel mass based on the number of bruised hepatic parenchyma voxel masses resulting from the removal of that vascular voxel mass;
- m function: calculation of the significance of a given portal vascular voxel mass based on the number of ischemic liver parenchymal voxel masses resulting from the removal of that vascular voxel mass.

(ii) Calculation of the importance of liver parenchymal voxel blocks:

- Living liver parenchyma: non-ischemic and bruised liver parenchyma;
- Dead liver parenchyma: ischemic or stagnant liver parenchyma;
- Base weights for two liver parenchyma: we defined the live liver parenchymal voxel block basis weight as d1 and the dead liver parenchymal voxel block basis weight as d2, defaulting to 0.5 for both;
- Vascular-related weights of liver parenchymal somatostatin masses: define as $\min\left(\mathrm{g}\left(p'_x\right),\mathrm{m}\left(p''_x\right)\right)$. Each liver parenchymal voxel block (x) takes the nearest hepatic vein voxel block and portal vein voxel block, respectively, as the hepatic/portal vein supply voxel block for that liver parenchymal voxel block (denoted by p'_x and p''_x, respectively). The vascular correlation weight of this liver parenchyma voxel block () is determined by the minimum value of $\mathrm{g}\left(p'_x\right)$ and $\mathrm{m}\left(p''_x\right)$. If the weight of the corresponding vascularized parenchymal voxel block is smaller, it means that the corresponding hepatic parenchymal voxel block is less important and can be removed more easily.

(iii) Calculation of the importance of the spatial unit based on the surface area of the cutting edge: the surface area weights w_S and the overall cut edge surface area change value ΔS of the voxel block if it is excised.

(iv) In summary, the weight function (Eq. [1]) is established, with the top two lines used to calculate the weights of the liver parenchyma voxel blocks and the bottom two lines used to calculate the weights of the vascular voxel blocks:

$$\mathrm{score}\left(x\right)=\begin{cases}\mathrm{w}_S\times\Delta s-\min\left(\mathrm{g}\left(p'_x\right),\mathrm{m}\left(p''_x\right)\right)+\mathrm{d1}, & \text{if } x \text{ is the substance of the living liver}\\ \mathrm{w}_S\times\Delta s-\min\left(\mathrm{g}\left(p'_x\right),\mathrm{m}\left(p''_x\right)\right)+\mathrm{d2}, & \text{if } x \text{ is dead liver parenchyma}\\ \mathrm{w}_S\times\Delta s-\mathrm{g}\left(x\right), & \text{if } x \text{ is the hepatic vein}\\ \mathrm{w}_S\times\Delta s-\mathrm{m}\left(x\right), & \text{if } x \text{ is the portal vein}\end{cases} \quad [1]$$

(III) Select the most weighted voxel to be excised and updated

Candidate voxels were identified along the resection margin using a weighted scoring function. The voxel with the highest score is selected as the proposed resection voxel. If the voxel is a hepatic parenchymal voxel mass, the vascular tree needs to be dynamically updated, and the resectable voxels neighboring the proposed resection voxel should be added to the candidate voxels and scored. If the voxel is a blood vessel, the ischemic stasis and vascular tree are updated, with the neighboring voxels being added to the candidate voxels and scored. This "Score-Select-Update"

© AME Publishing Company.

loop terminated when maximum voxel weight fell below zero.

Anatomical resection (AR) group in portal basin

ARs were simulated using a protocol integrating hepatic segmentation via portal-venous 3D reconstruction of the liver, voxelization, and vascular tree methods of the above study group.

NAR group with 1 cm margin

Based on the 3D liver model, NAR followed a 1-cm surgical margin protocol, same voxelization approach, and the same vascular tree methods.

Observation indicators

Voxel-based computational modeling was implemented across three surgical groups to quantify RI, II, CI, CRI, and TSR.

Statistical methods

SPSS 26.0 statistical software package (IBM Corp., Armonk, NY, USA) was used for data entry and statistical analysis. Continuous variables with normal distribution were expressed as expressed in $\bar{x}\pm s$, whereas non-normally distributed data were presented as median (lower quartile, upper quartile). Comparative analysis of the five volumetric parameters (RI, II, CI, CRI, and TSR) was conducted using the paired *t*-test for normally distributed data, and the Wilcoxon signed rank test for non-parametric data, with a significant P value of less than 0.05.

Results

A total of 140 liver space-occupying models were planned using three different methods, and the voxel model was used to calculate the five volumetric parameters (RI, II, CI, CRI, and TSR) (*Figure 5*). The statistical results did not follow a normal distribution, so the data were analyzed via Wilcoxon signed rank sum test (*Table 1*).

Ratio of resected liver parenchyma to total liver parenchyma volume

The RI in the study group was significantly lower than that in the AR group [8.09 (2.998, 20.115) *vs.* 18.900 (2.838, 42.285), P<0.05] but higher than that in the NAR group [8.09 (2.998, 20.115) *vs.* 1.980 (0.340, 3.055), P<0.05].

Ratio of remaining ischemic liver parenchyma volume to total liver parenchyma volume

The RI in the study group [1.145 (0.456, 3.426)] was greater than AR group baselines [0 (0–0), P<0.05] but remained below NAR group levels [7.628 (2.299, 24.159), P<0.05].

Ratio of remaining congested liver parenchyma volume to total liver parenchyma volume

The congested parenchyma ratio in the study group was less than that in the AR group [1.141 (0.368, 3.678) *vs.* 3.391 (0.352, 13.264), P<0.05] as well as less than that in the NAR group [1.141 (0.368, 3.678) *vs.* 7.668 (2.162, 22.982), P<0.05].

Ratio of remaining ischemic + congested liver parenchyma volume to total liver parenchyma volume

The composite ischemic + congested parenchyma ratio further confirmed therapeutic advantages, with the values in the study group significantly lower than those in the AR group [2.28 (0.824, 7.104) *vs.* 3.391 (0.352, 13.264), P<0.05] and the NAR group [2.28 (0.824, 7.104) *vs.* 15.28 (4.461, 47.141), P<0.05].

Sectional area of resected liver

Cross-sectional analysis of resection surfaces indicated that the study protocol achieved smaller liver cross-sectional area, compared to the AR protocol [14,417.13 (7,462.02, 32,715.68) *vs.* 73,739.52 (47,559.77, 102,632.74), P<0.05], but the cross-sectional area remained larger than that of the NAR group [14,417.13 (7,462.02, 32,715.68) *vs.* 6,613.897 (5,685.417, 13,560.409), P<0.05].

Discussion

In hepatic resection, it is crucial to preserve sufficient functional liver volume based on liver function after radical tumor resection (7,9,10). Although congested and ischemic liver parenchyma cannot be used as functional liver parenchyma, the surgical planning scheme in this study aimed to minimize the liver resection volume, residual congested liver volume, and ischemic volume to improve the safety of surgery. The choice of AR versus NAR mainly

© AME Publishing Company.

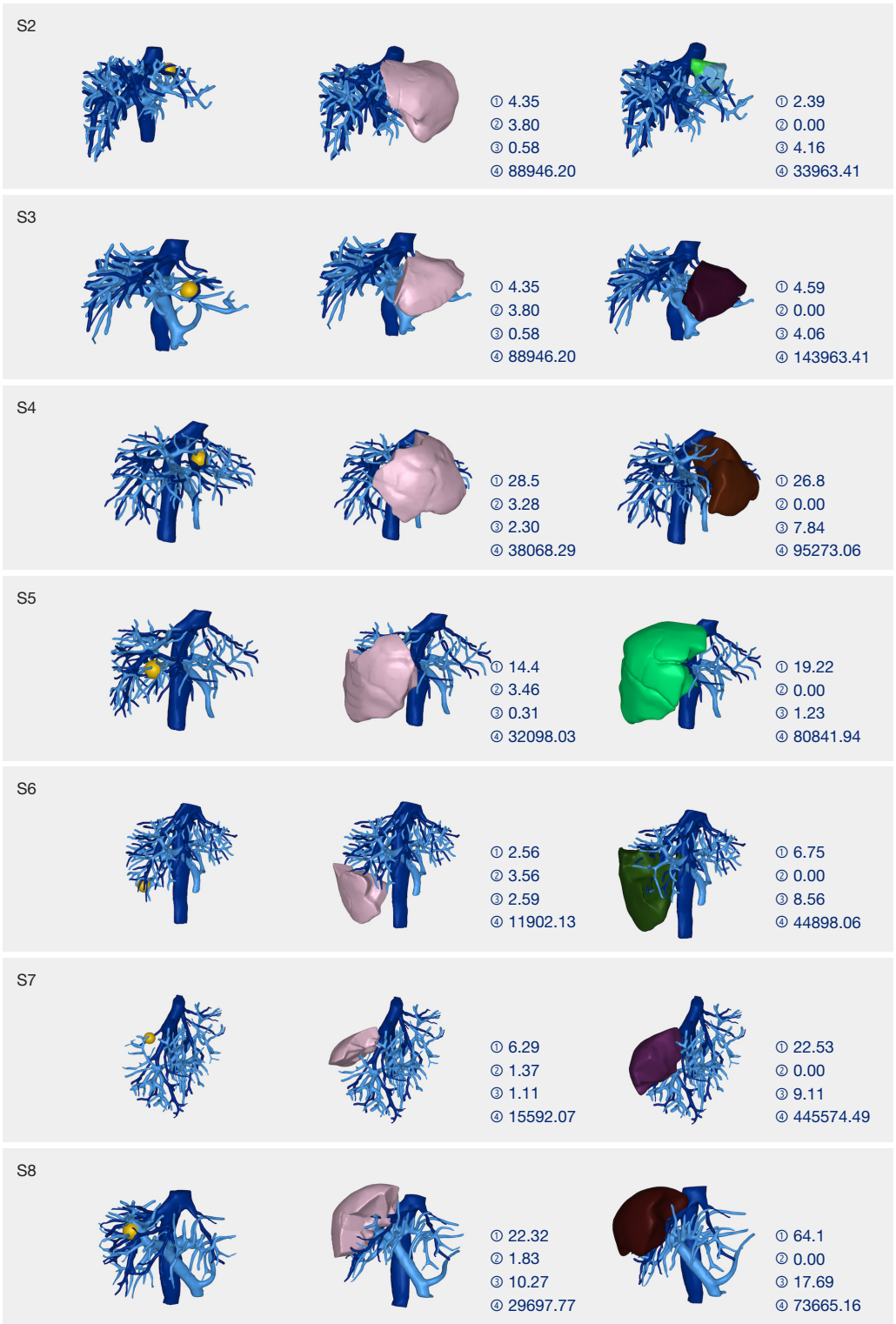

Figure 5 First column: occupied position; second column: hepatic resection in the study group; third column: anatomic hepatic resection (AR) in the portal basin. ①, volume of resected liver parenchyma/total liver parenchyma volume (%); ②, volume of remaining ischemic liver parenchyma/total liver parenchyma volume (%); ③, volume of remaining congested liver parenchyma/total liver parenchyma volume (%); ④, hepatic cross-sectional area (mm^2). AR, anatomical resection.

© AME Publishing Company.

Table 1 Wilcoxon signed rank sum test (N=420)

Observation indicators	Study group (n=140)	AR group (n=140)	NAR group (n=140)	Study *vs.* AR		Study *vs.* NAR	
				Z	P value	Z	P value
Resected liver parenchyma volume/ total liver parenchyma volume (ratio) (%)	8.090 (2.998, 20.115)	18.900 (2.838, 42.285)	1.980 (0.340, 3.055)	−5.054	<0.0001	−12.032	<0.0001
Remaining hepatic ischemic parenchymal volume/ total hepatic parenchymal volume (ratio) (%)	1.145 (0.456, 3.426)	0 (0, 0)	7.628 (2.299, 24.159)	−7.251	<0.0001	−13.062	<0.0001
Remaining hepatic congested parenchymal volume/ total hepatic parenchymal volume (ratio) (%)	1.141 (0.368, 3.678)	3.391 (0.352, 13.264)	7.668 (2.162, 22.982)	−8.284	<0.0001	−13.005	<0.0001
(Volume of remaining hepatic parenchyma ischemia + sludge)/ total hepatic parenchyma volume (ratio) (%)	2.28 (0.824, 7.104)	3.391 (0.352, 13.264)	15.28 (4.461, 47.141)	−7.792	0.006	−13.025	<0.0001
Sectional area of resected liver (mm^2)	14,417.129 (7,462.023, 32,715.685)	73,739.519 (47,559.775, 102,632.744)	6,613.897 (5,685.417, 13,560.409)	−12.895	<0.0001	−8.474	<0.0001

Data are presented as the median (lower quartile, upper quartile). AR, anatomical resection; NAR, non-anatomical resection.

depends on preoperative liver function and the presence of cirrhosis. Specifically, AR should be preferred to ensure tumor radicality, whereas NAR emerges as the preferred approach in patients with compromised liver function. This integrated approach combines the advantages of both resection modalities, including portal vein basin resection and a smaller liver parenchyma resection volume.

Some researchers have already focused on the reflux function of the hepatic vein (11,12). Wang *et al.* (13) incorporated the results of portal vein basin analysis and intraoperative indocyanine green fluorescence imaging to artificially determine the retention of all levels of inter-territory hepatic vein (IHV) in the basin of the loaded tumor intraoperatively with the dissection.

With the random number generation algorithm (6), this study simulated tumor distribution using seven randomly generated spherical lesions (1 cm diameter) per liver model, with strict exclusion criteria eliminating lesions within 1 cm of major portal/hepatic veins. Meanwhile, the planning effect of the research software can be tested more in a more reliable way.

One of the basic principles of hepatic resection is thoroughness, explicitly, complete resection of the tumor with no residual tumor at the margins. Currently, several regional guidelines recommend a margin of >1 cm for radical resection, and AR of the portal vein basin is also considered effective (14,15). The protocol strictly adheres to the international consensus guidelines (>1 cm margin). When more extensive portal vein basin resection is indicated, our algorithmic model enables strategic margin expansion through systematic adjustment of the initial surgical margin threshold. Moreover, the resection area was continuously expanded by simulated annealing, iterative greedy, and vascular tree algorithms at 1 mm^3 voxels, and concurrent minimization of five key parameters: RI, II, CI, CRI, and TSR.

Conventional anatomical liver resections focusing exclusively on the portal vein basin while ignoring the hepatic vein basin have been associated with residual liver congestion (16,17). Therefore, we included dual vascular basin analysis in the algorithm. Though the study group demonstrated greater residual ischemic volumes compared to AR controls, the ischemic plus congested liver volume of the study group was reduced significantly. Furthermore, the CV of the study group was less than that of the NAR group, achieving superior preservation of functional liver volume of the residual liver. This integration approach thereby increases the postoperative safety and reduces the

© AME Publishing Company.

risk of postoperative liver failure while ensuring the surgical outcome.

The TSA of the resected liver in hepatectomy is one of the important factors affecting the difficulty of surgery. A large cross-sectional area will undoubtedly increase the operation time and risk of intraoperative bleeding, postoperative liver bleeding, and bile leakage, which notably affects the safety of patients during surgery and postoperative recovery (18,19). Our algorithm incorporated TSA minimization as a critical constraint through 3D modeling, achieving significant TSA reduction, compared to the AR and NAR. These results suggest superior safety and convenience of the integrated approach relative to conventional segmentectomy, even compared to local resection.

Conclusions

This study establishes a novel hepatic resection planning framework through integration of coupled portal and hepatic vein basins, thereby achieving significant reduction in residual congested and ischemic liver volumes, as well as TSA. Furthermore, it provides new ideas for new personalized liver segmentation methods. The assessment criteria for the safety limit of hepatic resection consider both liver volume calculation and liver function (9). Therefore, the surgical planning scheme in this study can minimize congested and ischemic liver volume. Further investigation is necessary to determine whether more liver parenchyma can be resected compared with the previous assessment criteria for the safety limit of hepatic resection. With the integration of augmented reality navigation systems, our system may be applied to both preoperative planning and intraoperative navigation, thereby facilitating the achievement of truly precise hepatic resection.

Acknowledgments

None.

Footnote

Funding: This work was supported by the TCM Science and Technology Plan Project of Zhejiang Province (No. 2022ZB323); the Ningbo Municipal Key Research and Development Plan for 2023 (No. 2023Z210); the Medical and Health Science and Technology Plan Project of Zhejiang Province (No. 2022KY1114); the Medical Science and Technology Project of Zhejiang Province (No. 2024KY1499); the Clinical Research Fund Project of Zhejiang Medical Association (No. 2021ZYC-B24); and the Medical and Health Science and Technology Plan Project of Zhejiang Province (No. 2025KY1322).

Conflicts of Interest: All authors have completed the ICMJE uniform disclosure form (available at https://qims.amegroups.com/article/view/10.21037/qims-24-2349/coif). S.Y. reports that Ningbo Wedge Medical Technology Co., Ltd. provided data processing consulting services for this study. S.Y. is also a full-time employee of this company but declares that this relationship did not influence the research design, execution, or interpretation of results. The other authors have no conflicts of interest to declare.

Ethical Statement: The authors are accountable for all aspects of the work in ensuring that questions related to the accuracy or integrity of any part of the work are appropriately investigated and resolved. The study was conducted in accordance with the Declaration of Helsinki and its subsequent amendments. The study was approved by the Ethics Committee of The First Affiliated Hospital of Ningbo University (No. 2021-R138), and informed consent was provided by all participants.

Open Access Statement: This is an Open Access article distributed in accordance with the Creative Commons Attribution-NonCommercial-NoDerivs 4.0 International License (CC BY-NC-ND 4.0), which permits the non-commercial replication and distribution of the article with the strict proviso that no changes or edits are made and the original work is properly cited (including links to both the formal publication through the relevant DOI and the license). See: https://creativecommons.org/licenses/by-nc-nd/4.0/.

References

1. Xie Y, Hu W, Cai S. Observation on the course and distribution of the right posterior branch of portal vein in 100 cases. J Hepatopancreatobiliary Surg 2011;23:283-5.
2. Takasaki K. Glissonean pedicle transection method for hepatic resection: a new concept of liver segmentation. J Hepatobiliary Pancreat Surg 1998;5:286-91.
3. Cho A, Okazumi S, Takayama W, Takeda A, Iwasaki K, Sasagawa S, Natsume T, Kono T, Kondo S, Ochiai T, Ryu M. Anatomy of the right anterosuperior area (segment 8) of the liver: evaluation with helical CT during arterial

portography. Radiology 2000;214:491-5.
4. Majno P, Mentha G, Toso C, Morel P, Peitgen HO, Fasel JH. Anatomy of the liver: an outline with three levels of complexity--a further step towards tailored territorial liver resections. J Hepatol 2014;60:654-62.
5. Torzilli G, Garancini M, Donadon M, Cimino M, Procopio F, Montorsi M. Intraoperative ultrasonographic detection of communicating veins between adjacent hepatic veins during hepatectomy for tumours at the hepatocaval confluence. Br J Surg 2010;97:1867-73.
6. Matsumoto M, Nishimura T. Mersenne twister: a 623 dimensionally equidistributed uniform pseudo-random number generator. ACM Trans Model Comput Simul 1998;8:3-30.
7. Cerreto M, Cardone F, Cerrito L, Stella L, Santopaolo F, Pallozzi M, Gasbarrini A, Ponziani FR. The New Era of Systemic Treatment for Hepatocellular Carcinoma: From the First Line to the Optimal Sequence. Curr Oncol 2023;30:8774-92.
8. Jin S, Lewis R, West D. A comparison of algorithms for vertex normal computation. Vis Comput 2005;21:71-82.
9. Makuuchi M, Hasegawa H, Yamazaki S. Indication for hepatectomy in patients with hepatocellular carcinoma and cirrhosis. Shindan to Chiryo 1986;74:1225-30.
10. DuBray BJ Jr, Chapman WC, Anderson CD. Hepatocellular carcinoma: a review of the surgical approaches to management. Mo Med 2011;108:195-8.
11. Fang C, An J, Bruno A, Cai X, Fan J, Fujimoto J, et al. Consensus recommendations of three-dimensional visualization for diagnosis and management of liver diseases. Hepatol Int 2020;14:437-53.
12. Kaibori M, Chen YW, Matsui K, Ishizaki M, Tsuda T, Nakatake R, Sakaguchi T, Matsushima H, Miyawaki K, Shindo T, Tateyama T, Kwon AH. Novel liver visualization and surgical simulation system. J Gastrointest Surg 2013;17:1422-8.
13. Wang X, Li J, Cao J, Zhang Q, Wei Y, Cheng W, Liang X, Tian F, Wang X, Xu H, Chen J, Zhou N, Yang Z, Tao C, Wang H. Approaches of laparoscopic anatomical liver resection of segment 8 for hepatocellular carcinoma: a retrospective cohort study of short-term results at multiple centers in China. Int J Surg 2023;109:3365-74.
14. EASL Clinical Practice Guidelines: Management of hepatocellular carcinoma. J Hepatol 2018;69:182-236.
15. Kudo M, Kawamura Y, Hasegawa K, Tateishi R, Kariyama K, Shiina S, et al. Management of Hepatocellular Carcinoma in Japan: JSH Consensus Statements and Recommendations 2021 Update. Liver Cancer 2021;10:181-223.
16. Orozco G, Gupta M, Villagomez D, Shah M, Marti F, Mei X, Ancheta A, Desai S, Salama F, Benrajab K, Davenport D, Gedaly R. Predictors of Liver Failure in Non-Cirrhotic Patients Undergoing Hepatectomy. World J Surg 2022;46:3081-9.
17. Wang J, Zhang Z, Shang D, Liao Y, Yu P, Li J, Chen S, Liu D, Miao H, Li S, Zhang B, Huang A, Liu H, Zhang Y, Qi X. A Novel Nomogram for Prediction of Post-Hepatectomy Liver Failure in Patients with Resectable Hepatocellular Carcinoma: A Multicenter Study. J Hepatocell Carcinoma 2022;9:901-12.
18. Okamura Y, Yamamoto Y, Sugiura T, Ito T, Ashida R, Ohgi K, Uesaka K. Novel patient risk factors and validation of a difficulty scoring system in laparoscopic repeat hepatectomy. Sci Rep 2019;9:17653.
19. Xi C, Zhu M, Ji T, Tan Y, Zhuang L, Yuan Z, Zhang Z, Xu L, Liu Z, Xu X, Xue W, Ding W. A novel difficulty scoring system of laparoscopic liver resection for liver tumor. Front Oncol 2022;12:1019763.

Cite this article as: Zhang M, Peng C, Zhao Y, Hong Y, Zhu G, Ying S, Zhang B, Ren X, Zhu J, Zheng J, Yu Z, Chen Y, Zheng S. A precise surgical planning system for hepatectomy coupled with liver tissue in the hepato-portal vein territories. Quant Imaging Med Surg 2025;15(5):3839-3848. doi: 10.21037/qims-24-2349

© AME Publishing Company.